

Nucleon isovector tensor charge from lattice QCD with physical light quarks

Ryutaro TSUJI^{1,2}, Yasumichi AOKI², Ken-Ichi ISHIKAWA³, Yoshinobu KURAMASHI⁴, Shoichi SASAKI¹, Eigo SHINTANI⁴ and Takeshi YAMAZAKI^{4,5}

(PACS Collaboration)

¹*Department of Physics, Tohoku University, Sendai 980-8578, Japan*

²*RIKEN Center for Computational Science, Kobe 650-0047, Japan*

³*Core of Research for the Energetic Universe, Graduate School of Advanced Science and Engineering, Higashi-Hiroshima 739-8526, Japan*

⁴*Center for Computational Science, University of Tsukuba, Tsukuba 305-8577, Japan*

⁵*Faculty of pure and Applied Science, University of Tsukuba, Tsukuba 305-8571, Japan*

E-mail: tsuji@nucl.phys.tohoku.ac.jp

(Received January, 17, 2022)

We present preliminary results for the axial, scalar and tensor charges of the nucleon measured in 2+1 flavor QCD with the physical light quarks ($m_\pi = 135$ MeV). Our simulations are carried out with gauge configurations generated by the PACS Collaboration with the stout-smear $O(a)$ improved Wilson fermions and Iwasaki gauge action at a single lattice spacing of 0.085 (fm). There are two lattice ensembles of the PACS gauge configurations, which have physical lattice sizes over $(10 \text{ fm})^4$ and $(5 \text{ fm})^4$, respectively. We compute the nucleon three-point correlation functions in the axial, scalar, and tensor channels. For the renormalization, we use the Rome-Southampton method as the intermediate scheme in order to evaluate the renormalization constants for the scalar and tensor currents in fully nonperturbative manner. We then evaluate the renormalized values of the scalar and tensor charges (g_S and g_T) in the $\overline{\text{MS}}$ scheme at the renormalization scale of 2 GeV with a help of the continuum perturbation theory for the matching between two schemes. We compare our preliminary results of g_S and g_T with those of other collaboration results.

KEYWORDS: Nucleon structure, Lattice QCD, ...

1. Introduction

In the standard model of modern particle physics, the nucleon is known to be a composite particle made of quarks and gluons, and their interactions are described by QCD. Due to the nonperturbative nature of QCD at low energy scales, the nucleon structure that is governed by strong many body problem of the elementary constituents is one of the great challenges of lattice QCD. Future and current precision β -decay measurements with cold and ultracold neutrons provides us an opportunity to study the sensitivity of the nucleon isovector matrix elements to new physics beyond the standard model (BSM). The neutron life-time puzzle is one of such examples [1]. The discrepancy between the results of beam experiments and storage experiments remains unsolved. It is still an open question that deserves further investigation in terms of the nucleon axial charge (g_A). Although the nucleon axial charge dominates the weak decay of the neutron, there is no reason to forbid the other channel contributions to the neutron decay if the BSM contributions are present. In this sense, the scalar and tensor charges (g_S and g_T), which are less known experimentally, play important roles to constrain the limit of non-standard interactions [2–4].

2. Method

The axial, tensor and scalar charges can be evaluated from the nucleon matrix element of a given bilinear operator, $O_\Gamma = \bar{\psi}\Gamma\psi$ with $\Gamma = \gamma_5\gamma_i$, 1 and $\gamma_i\gamma_j (i \neq j)$, respectively.

In general, the nucleon matrix elements are evaluated from a ratio of the nucleon three-point function with a given operator O_Γ inserted at $t = t_{\text{op}}$ being subject to a range of $t_{\text{snk}} > t > t_{\text{src}}$, to the nucleon two-point function with a source-sink separation ($t_{\text{sep}} = t_{\text{snk}} - t_{\text{src}}$) as

$$R(t_{\text{sep}}, t_{\text{op}}) \equiv \frac{C^{\text{3pt}}(t_{\text{op}}, t_{\text{sep}})}{C^{\text{2pt}}(t_{\text{sep}})} \xrightarrow{t_{\text{sep}} \gg t_{\text{op}} \gg 0} \langle 1|O_\Gamma|1 \rangle + \mathcal{O}(e^{-t_{\text{sep}}\Delta}) + \mathcal{O}(e^{-(t_{\text{sep}}-(t_{\text{op}}-t_{\text{src}})\Delta)}), \quad (1)$$

where $|i\rangle$ represents the i -th energy eigenstate and $i = 1$ stands for the ground state of the nucleon. If the condition $t_{\text{sep}} \gg t_{\text{op}} - t_{\text{src}} \gg 0$ is satisfied, the desired matrix element $\langle 1|O_\Gamma|1 \rangle$ can be read off from an asymptotic plateau, which is independent of a choice of t_{op} . Narrower source-sink separation causes systematic uncertainties stemming from the excited states contamination represented by two terms of $\mathcal{O}(e^{-t_{\text{sep}}\Delta})$ and $\mathcal{O}(e^{-(t_{\text{sep}}-(t_{\text{op}}-t_{\text{src}})\Delta})$, where $\Delta \equiv E_2 - E_1$ denotes a difference between the two energies of the ground state (E_1) and the lowest excited state (E_2).

In this study, the nucleon interpolating operator is constructed by the exponentially smeared quark operators, so as to maximize an overlap with the nucleon ground state as

$$N(t, \vec{p}) = \sum_{\vec{x}_1, \vec{x}_2, \vec{x}_3} e^{-i\vec{p}\cdot\vec{x}} \varepsilon_{abc} \left[u_a^T(t, \vec{x}_1) C \gamma_5 d_b(t, \vec{x}_2) \right] u_c(t, \vec{x}_3) \times \prod_{i=1}^3 A \exp(-B|\vec{x}_i - \vec{x}|) \quad (2)$$

where there are two smearing parameters (A, B). Since the condition, $t_{\text{sep}} \gg t_{\text{op}} \gg 0$ appearing in Eq. (1) is usually not satisfied in practice, the excited states contaminations could not be fully eliminated by tuning smearing parameters. For the purpose of eliminating the systematic uncertainties, one should calculate the ratio (1) with several choices of t_{sep} , and then makes sure whether the evaluated value of the nucleon matrix element does not change with a variation of t_{sep} within a certain precision. This is called the ratio method that is mainly used in this study.

In order to compare with the experimental values or other lattice results, the *bare matrix elements* obtained from the above mentioned method should be renormalized with the renormalization constants Z_{O_Γ} for each Γ operator in a certain scheme. The Rome-Southampton method, which is known as the Regularization Independent (RI) scheme, is often used as the intermediate scheme in order to evaluate the renormalization constants Z_{O_Γ} in fully nonperturbative manner. The resulting renormalization constants are then converted to the $\overline{\text{MS}}$ scheme at certain scale μ_0 and evolved to the scale of 2 GeV using the perturbation theory.

In general, the final result of $Z_{O_\Gamma}^{\overline{\text{MS}}}(2\text{GeV})$ receives the residual dependence of the choice of the matching scale μ_0 . The perturbative conversion from the RI scheme to the $\overline{\text{MS}}$ scheme produces the residual μ_0 dependence. There are two main sources as follows. One stems from lattice discretization errors at higher μ_0 , while another is originated from the nonperturbative effect that becomes relevant at lower μ_0 [12]. The latter becomes serious when the physical lattice volume gets larger. However, as pointed out in Ref. [12], if a Symmetric MOMentum subtraction point is adopted in the RI scheme (hereafter regarded as the RI/SMOM scheme), the infrared effect is highly suppressed. In this paper, we use the RI/SMOM scheme for this purpose. In order to reduce the systematic uncertainties associated with the residual μ_0 -dependence, we used following two types of fitting functional forms as functions of the matching scale μ_0

$$f_{O_\Gamma}^{\text{Global}}(\mu_0) = \frac{c_{-1}}{(\Lambda^{-1}\mu_0)^2} + c_0 + \sum_{k>0}^{k_{\text{max}}} c_k (a\mu_0)^{2k} \quad \text{and} \quad f_{O_\Gamma}^{\text{IR-trunc.}}(\mu_0) = c_0 + \sum_{k>0}^{k_{\text{max}}} c_k (a\mu_0)^{2k} \quad (3)$$

with c_0 being the μ_0 -independent value of $Z_{O_F}^{\overline{\text{MS}}}(\mu)$ at the renormalization scale $\mu = 2$ GeV. The former functional form includes the term of the negative power of μ_0 , which is induced by the nonperturbative effect characterized by a scale Λ . Therefore, the former is applied for fitting all data (denoted as ‘‘Global’’ in superscript), while the latter functional form is used for fitting the data in a restricted range of $\mu_0 \geq \mu$ (denoted as ‘‘IR-trunc.’’ in superscript). The value of k_{max} is determined by a χ^2 test for goodness fit, so that $k_{\text{max}} = 1$ and 2 are chosen in each case. The discrepancy on the values of c_0 extracted from these fittings with $k_{\text{max}} = 1, 2$ is quoted as a systematic error on the renormalization constant.

3. Simulation details

We mainly use the PACS10 configurations generated by the PACS Collaboration with the six stout-smear $O(a)$ improved Wilson-clover quark action and Iwasaki gauge action at $\beta = 1.82$ corresponding to the lattice spacings of 0.085 fm [7–11] with physical light quarks. When we compute nucleon two- and three-point functions, the all-mode-averaging (AMA) technique [13] is employed in order to reduce the statistical errors significantly without increasing computational costs. Two lattice ensembles are generated with the same lattice spacing, but on different lattice sizes: $L^3 \times T = 128^3 \times 128$ and $64^3 \times 64$ corresponding $(10.9 \text{ fm})^4$ and $(5.5 \text{ fm})^4$ lattice volumes. The smaller volume ensemble is used for the finite volume study on the g_A and nucleon elastic form factors, and also used for computing the renormalization constants which are known to be less sensitive to the finite volume effect.

Table I. Details of the measurements: lattice size, time separation (t_{sep}), the smearing parameters (A, B), the number of high-precision calculation (N_{org}), the number of configurations (N_{conf}), the measurements per configuration (N_G) and the total number of the measurements ($N_{\text{meas}} = N_{\text{conf}} \times N_G$), respectively.

Lattice size	t_{sep}/a	Smearing parameters	N_{org}	N_G	N_{conf}	N_{meas}
128^4 lattice	10	$(A, B) = (1.2, 0.16)$	1	128	20	2,560
	12		1	256	20	5,120
	14		2	320	20	6,400
	16		4	512	20	10,240
64^4 lattice	11	$(A, B) = (1.2, 0.16)$	4	40	50	2,000
	14		4	64	100	6,400
	12	$(A, B) = (1.2, 0.14)$	4	256	100	25,600
	14		4	1,024	100	102,400
	16		4	2,048	100	204,800

4. Numerical results

In this study, we present the preliminary results for the renormalized values of the isovector axial, scalar and tensor charges. All of the *bare matrix elements* are evaluated with both 128^4 and 64^4 lattice ensembles. As for the renormalization, the local vector and axial currents are renormalized with the value of $Z_V = 0.9513(76)(1487)$ and $Z_A = 0.9650(68)(95)$ obtained by the Schrödinger functional scheme at the vanishing quark mass [14], while the renormalization constants for the scalar and tensor charges are evaluated with RI/SMOM scheme as described in Sec.2.

In Fig 1, we show the t_{sep} dependence of g_A, g_S and g_T , which are evaluated with the ratio method. The error bars for g_A and the inner errors for g_S and g_T represent their statistical errors, while the outer ones represent the total error including the systematic error stemming from the renormalization.

According to the analysis based on the ratio method, it is found that the condition $t_{\text{sep}} > 1$ (fm) is enough to suppress the excited states contaminations in all three channels.

We compare our preliminary results of the renormalized values of g_S (left) and g_T (right) together with results from the recent lattice QCD calculations in Fig 2. Remark that our results are obtained solely from the physical point simulations which suffer from large statistical fluctuations, while the other lattice results are given by the combined data that includes the data taken from simulations at the heavier pion masses. However, the statistical and total errors on our results are comparable to the other lattice results, since we use the AMA method for the bare matrix elements and the RI/SMOM scheme for the renormalization, both of which reduce the statistical and systematic uncertainties on the final results. As for g_S , our preliminary result is consistent with the trend of the other results. On the other hand, our result of g_T locates slightly higher than other continuum results, though this discrepancy would be caused by the discretization uncertainty that is not yet accounted in our calculations.

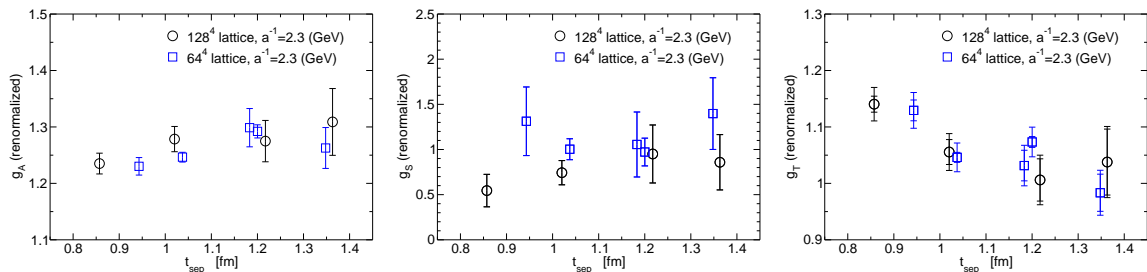


Fig. 1. t_{sep} dependence of the renormalized values of g_A (left), g_S (center) and g_T (right). The horizontal axis denotes the source-sink separation t_{sep} in physical unit. The inner and outer error bars represent their statistical and total uncertainties, respectively.

5. Summary

We have calculated the renormalized values of the nucleon isovector charge in the axial, scalar and tensor channels using 2+1 flavor lattice QCD with physical light quarks. The calculations are carried out with the gauge configurations generated by the PACS Collaboration. In order to achieve high-precision and high-accuracy determination, we employ the AMA technique which can reduce the statistical error significantly, and the RI/SMOM scheme which keeps the systematic error under control. Consequently, we precisely determined g_S and g_T only at the physical point. Our results are comparable to the other lattice results, though the discretization uncertainties are not yet evaluated. Our research continues at a second, finer spacing ($a = 0.064$ fm), and is now in progress [15].

Acknowledgement

Numerical calculations in this work were performed on Oakforest-PACS in Joint Center for Advanced High Performance Computing (JCAHPC) and Cygnus in Center for Computational Sciences at University of Tsukuba under Multidisciplinary Cooperative Research Program of Center for Computational Sciences, University of Tsukuba, and Wisteria/BDEC-01 in the Information Technology Center, The University of Tokyo. This research also used computational resources through the HPCI System Research Projects (Project ID: hp170022, hp180051, hp180072, hp180126, hp190025, hp190081, hp200062, hp200188, hp210088) provided by Information Technology Center of the University of Tokyo and RIKEN Center for Computational Science (R-CCS). The calculation employed OpenQCD system(<http://luscher.web.cern.ch/luscher/openQCD/>). This work was supported in part

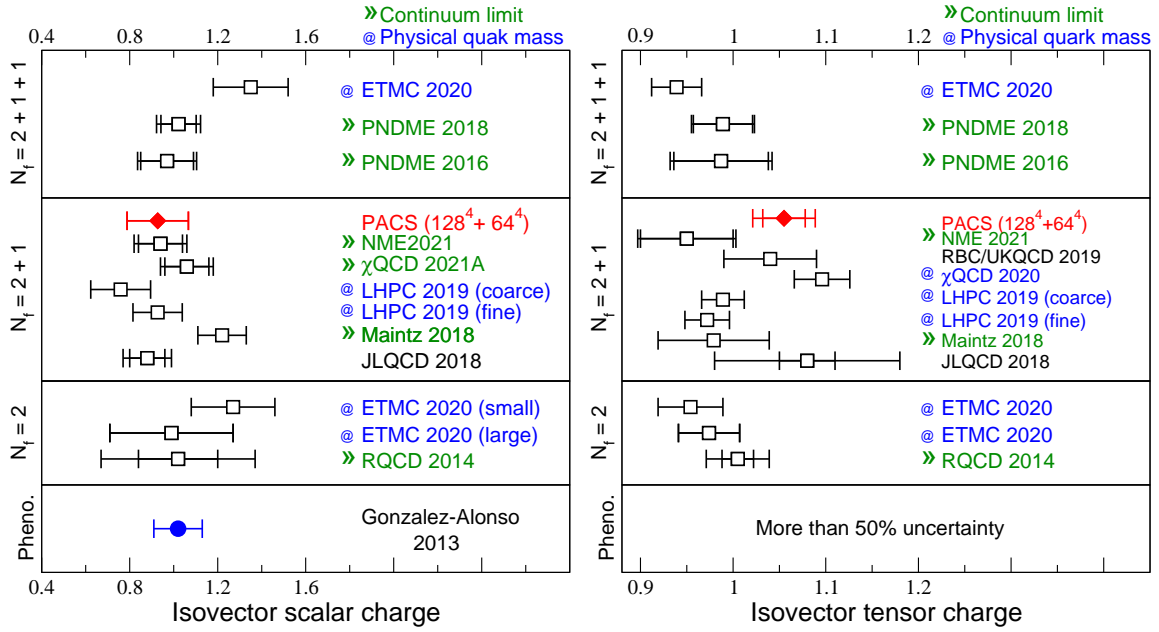


Fig. 2. Comparison of our preliminary results (red diamonds) with the other lattice results (black squares) and the phenomenological value (blue circle) [5,6] for g_S (left panel) and g_T (right panel). The inner error bars represent the statistical uncertainties, while the outer ones represent the total uncertainties given by adding the statistical and systematic errors in quadrature. Blue labels indicate that the analysis includes the data from lattice QCD simulation near the physical point, while green labels indicate that the continuum extrapolation is achieved.

by Grants-in-Aid for Scientific Research from the Ministry of Education, Culture, Sports, Science and Technology (Nos. 18K03605, 19H01892). This work was supported by RIKEN Junior Research Associate Program.

References

- [1] A. Czaeński, W. J. Marciano and A. Sirin, Phys. Rev. Lett. **120**, no.20, 202002 (2018).
- [2] T. Bhattacharya, V. Cirigliano, S. D. Cohen, A. Filipuzzi, M. Gonzalez-Alonso, M. L. Graesser, R. Gupta and H. W. Lin, Phys. Rev. D **85**, 054512 (2012).
- [3] A. Courtoy, S. Baeßer, M. González-Alonso and S. Liuti, Phys. Rev. Lett. **115**, (162001 (2015).
- [4] V. Cirigliano, S. Gardner and B. Holstein, Prog. Part. Nucl. Phys. **71**, 93-118 (2013).
- [5] For review of g_S and g_T , see Y. Aoki, T. Blum, G. Colangelo, S. Collins, M. Della Morte, P. Dimopoulos, S. Dürr, X. Feng, H. Fukaya and M. Golterman, *et al.* [arXiv:2111.09849 [hep-lat]] and references therein.
- [6] M. González-Alonso and J. Martin Camalich, Phys. Rev. Lett. **112**, no.4, 042501 (2014).
- [7] K. I. Ishikawa *et al.* (PACS), Phys. Rev. D **99** (2019) 014504, arXiv:1807.06237 [hep-lat].
- [8] K. I. Ishikawa *et al.* (PACS), Phys. Rev. D **100** (2019) 094502.
- [9] E. Shintani *et al.*, Phys. Rev. D **94** (2019) 014510. (Erratum; Phys. Rev. D **102** (2020) 019902.)
- [10] K. I. Ishikawa *et al.* [PACS], Phys. Rev. D **104**, no.7, 074514 (2021).
- [11] Y. Taniguchi, PoS LATTICE2012, 236 (2012), arXiv:1303.0104 [hep-lat].
- [12] Y. Aoki, P. A. Boyle, N. H. Christ *et al.*, Phys. Rev. D **78** (2008) 054510.
- [13] T. Blum, T. Izubuchi, and E. Shintani, Phys. Rev. D **88** (2013) 094503.
- [14] K. I. Ishikawa *et al.* (PACS), PoS LATTICE2015 (2016) 271.
- [15] R. Tsuji *et al.* (PACS), arXiv:2112.15276 (2021).